Influence of combined effect of dopant and capping agent on Structural, Optical Electrochemical properties of Zinc Sulphide quantum dots

[1]S. Velusubhash, [2]K. Kalirajan, [3]S. Harikengaram, [4]R. Vettumperumal, [5]R. Murugesan,
[1]Research Scholar, PG and Research Department of Chemistry, Sri Paramakalyani College affliated to Manonmaniam Sundaranar University, Abishekapatti, Tirunelveli – 627 012, Tamil Nadu, India.
[2]PG and Research Department of Chemistry, Sri Paramakalyani College, Alwarkurichi, Tirunelveli – 627 412, Tamilnadu, India.
[3]PG Department of Chemistry, Pasumpon Muthuramalinga Thevar College, Melaneelithanallur, Tirunelveli – 627 953, Tamilnadu, India.
[4]Department of Physics, V V College of Engineering, Tisaiyanvilai, Tirunelveli – 627 657, Tamilnadu, India.
[5]Department of Chemistry, T.D.M.N.S. College, T.Kallikulam, Tirunelveli – 627113, Tamilnadu, India.

Abstract: In the present work, the combined effect of dopant and capping agent on Zinc sulphide (ZnS) Quantum dots (QDs) has taken for investigation. Simple chemical co- precipitation technique has been employed for preparing the ZnS QDs samples. The transition metal of Nickel ion (Ni^{2+}) is used as a dopant, Urea and thiourea are used as capping agents for preparation of ZnS QDs samples at room temperature. Pure ZnS QDs and Ni^{2+} ion doped ZnS QDs in different capping agent were characterized by UV-Visible, FTIR, PL, XRD, SEM, EDAX and Electrochemical workstation. The XRD investigations indicated that the prepared undoped and doped ZnS QDs samples with different capping agents are crystalline, with cubic zinc blend structure. ZnS QDs samples exhibits an crystallite size of 1.2 to 1.8 nm. FTIR analysis confirms the inclusion of Ni^{2+} dopant along with different capping agent such as urea and thiourea into ZnS QDs. UV- Visible analysis showed a broad adsorption band around 293-305 nm. The blue-shift in the absorption spectra and corresponding variation in band gap were also observed. The PL investigations showed narrow and sharp emission band at around 388 nm, 522 nm and 789 nm. Electrochemical analysis was carried out by studying the transition of photogenerated electrons in all the ZnS QDs samples with modified Glassy carbon electrodes (GCE). In addition, the prepared ZnS QDs samples were used as nanophotocatalysts, for photodegradation of Malchite Green (MG) dye. Urea capped Ni^{2+} doped ZnS QDs act as a better photocatalyst under visible light radiation.

IndexTerms **- Quantum dots, Dopant, Capping agent, Band gap, Photo catalyst.**

I. INTRODUCTION

Among semiconductor materials, ZnS QDs occupies a significant position in field of nanomaterials. ZnS QDs exhibit quantum confinement effects and surface effects [1]. Quantum confinement effect modifies the electronic structure of the ZnS when their sizes are comparable to that of the Bohr excitonic radius of respective materials [2]. Surface states will play a more important role in the QDs, due to their large surface-to-volume ratio with a decrease in particle size [3]. In the case of semiconductor QDs, radiative and non radiative transition of an exciton at the surface states becomes dominant or eliminated with a decrease or increase of particle size [4]. Elimination of recombination of electron hole pair may be due to the creation of traps for electron or holes on the surface of the catalyst. Therefore, the trapping of an electron and hole at the surface states have influence the qualities of the material for an optoelectronic device [5]. These size-dependent optical properties have many potential applications in the areas of solar energy conversion, light-emitting devices, chemical/biological sensors, and photocatalysis. Hence it can display novel structural, optical, electronic, magnetic and chemical properties that can be used for many important technological applications [6, 7]. Current trend in field of QDs is to find different ways to control size and morphology of the QDs, since their properties and applications are size and morphology dependent to the larger extent [8].

The increased surface area to volume ratio creates surface states, which alters the activity of electrons and hole which influences the chemical reaction dynamics [9]. Therefore, nanostructures such as ZnO [10], carbon nanotubes [11], CdO [12, 13], CdS [14], ZnS NPs [15], CdSe NPs [16], GaN nanowires [17] etc. are intensively investigated for their prospective applications. ZnS is one of the first discovered II–VI compound semiconductor materials with flexible fundamental properties. Due to its wide band-gap of 3.54 eV, ZnS is widely used as phosphor and heterogeneous photo-catalyst [18]. ZnS QDs have attracted great interest of researchers due to their excellent size tunable optical properties. It has been reported that inclusion of dopant metal and capping material in ZnS QDs lattice modify the optical transition efficiencies of carriers and increases the number of optically active sites [19]. Novel luminescence characteristics, such as stable, fast and intense visible light emission with different colours have been noticed from doped ZnS QDs [20].

Doped materials show different types of luminescent properties which are strongly depended on the type of dopant ions [21]. There are several reports on the photoluminescence properties of ZnS nanostructures doped by different impurities namely Cu^{2+}, Mn^{2+}, Co^{2+}, Ni^{2+} rare earth and transition elements etc [22] occupying Zn lattice site and behaves as a trap site for electron and holes.

Semiconductor QDs are themselves highly unstable in the absence of a trapping medium they agglomerate or coalesce extremely quickly. For this reason, the bonding of capping agents to the QDs is necessary to provide surface passivation and also to improve the surface state, which significantly tune the optoelectronic characteristics of QDs [23, 24]. In general, the agglomeration can be arrested by two factors: first, electrostatic stabilization and second, inducing steric hindrances [25]. An important application of ZnS QDs in photocatalysis is due to the rapid generation of electron–hole pairs by photoexcitation and the highly negative reduction potentials of excited electrons [24]. Also, these QDs show good photocatalytic activity due to trapped holes arising from surface defects on the sulphides making them a suitable material to use as a photocatalyst.

In the present study, the combined effect of capping agent namely urea and thiourea in Ni^{2+} ion dopant on ZnS QDs has been studied. The effect of doping along with capping agent on crystallite size, morphology, photoluminescence, electrochemical properties and photo-catalytic activity has been studied. To the best of our knowledge, present paper is the first report mentioning the photo-catalytic activity of as prepared undoped ZnS QDs, Ni (3%) doped ZnS QDs (ZnS QDs: Ni(3%)), Urea capped Ni(3%) doped ZnS QDs (ZnS QDs: Ni(3%), Urea), Thiourea capped Ni(3%) doped ZnS QDs (ZnS QDs: Ni(3%), Thio Urea) over MG dye.

2. 2. Experimental methods

2.1. Materials

Zinc acetate dehydrate ($Zn(CH_3COO)_2.2H_2O$), Nickel Chloride (II) hexa hydrate ($NiCl_2.6H2O$), Thiourea and Urea were purchased from Hi Media and used without further purification, sodium sulphide (Na_2S) were purchased from Hi-Media, India with high purity (99.99%), Water was used after two distillations (DDW).

2.2. Synthesis

2.2.1. Preparation of ZnS QDs

ZnS QDs were prepared by chemical precipitation method. In a typical procedure, 2.0 M of $Zn(CH_3COO)_2.2H_2O$ in 50ml of deionized water and 2.0 M of sodium sulphide in 50 ml of deionized water were mixed drop by drop. The solution was heated about 80ºC under magnetic stirring for 2 hours. The precipitate was collected and washed several times with deionized water and ethanol. The precipitate was dried in a hot air oven at 120ºC for 6 hours, ground to obtain ZnS QDs.

2.2.2. Preparation of ZnS: Ni (3%) QDs

Ni (3%) doped ZnS QDs samples were prepared by chemical precipitation method. 1.94 M $Zn(CH_3COO)_2.2H_2O$ and 0.06M $NiCl_2.6H_2O$ were dissolved (Zn:Ni =0.97:0.03, in mol) in 50 ml of distilled water, stirred for 10 min. And then 2.0 M Sodium sulfide aqueous solution was added to the above solution mixture drop-by-drop under magnetic stirring. The solution was maintained at 80ºC under continued stirring for 2 hours. The precipitate was washed with de-ionised water and ethanol for several times. The precipitate was dried for 6 hours at 120ºC and ground to obtain Ni (3%) doped ZnS QDs sample.

2.2.3. Preparation of Thiourea capped ZnS: Ni (3%) QDs

Thiourea capped Ni (3%) doped ZnS QDs samples were prepared by chemical precipitation method. 1.94 M $Zn(CH_3COO)_2.2H_2O$ and 0.06M $NiCl_2.6H_2O$ were dissolved (Zn:Ni =0.97:0.03, in mol) in 50 ml of distilled water, stirred for 10 min. And then 2.0 M Sodium sulfide aqueous solution was added to the above solution mixture drop-by-drop under constant magnetic stirring. An appropriate amount of Thiourea (0.5 g) was also added to the reaction medium to stabilize the particle surfaces. The solution was maintained at the temperature of 80ºC under continued stirring for 2 hours. The precipitate was washed with de-ionised water and ethanol for several times. The precipitate was dried for 6 hours at 120ºC and ground to obtain Thio urea capped Ni (3%) doped ZnS QDs sample.

2.2.4. Preparation of urea capped ZnS: Ni (3%) QDs

Urea capped Ni (3%) doped ZnS QDs samples were prepared by chemical precipitation method. 1.94 M $Zn(CH_3COO)_2.2H_2O$ and 0.06M $NiCl_2.6H_2O$ were dissolved (Zn:Ni =0.97:0.03, in mol) in 50 ml of distilled water, stirred for 10 min. And then 2.0 M Sodium sulfide aqueous solution was added to the above solution mixture drop-by-drop under constant magnetic stirring. An appropriate amount of urea (0.5 g) was also added to the reaction medium to stabilize the particle surfaces. The solution was maintained at the temperature of 80ºC under continued stirring for 2 hours. The precipitate was washed with de-ionised water and ethanol for several times and centrifuged. The precipitate was dried for 6 hours at 120ºC and ground to obtain Urea capped Ni (3%) doped ZnS QDs sample.

2.3 Characterization Techniques

The prepared samples were characterized by X-ray diffractometer (XRD 6000, shimadzu Analytical, Japan) with Cu-Kα radiation source (λ=1.54 A) operated at 40 kV and 30 mA in the 2θ range 10-90º at the scan speed of 10.0º per minute for structural analysis. Surface morphological and Elemental analysis of prepared samples was done by using SEM (JSM 6390, JEOL, USA) equipped with EDAX (INCA, Oxford). FTIR spectra for the samples were recorded by using FTIR-410 spectrophotometer (JASCO, Texas, USA) in the wavenumber region 4000-400 cm^{-1}. Optical absorption spectra have been recorded with the help of UV-Visible spectrophotometer (JASCO, Japan) in the range of 200 to 800 nm. Photoluminescence (PL) measurements were performed at room temperature in a spectrofluorometer (LS-55, Perkin-Elmer, USA) equipped with a Xenon lamp. The samples were dispersed in ethanol solvent, excited with excitation wavelengths of 330 nm and the spectra were recorded ranging from 300 nm to 900 nm. The electrochemical experiments were carried out to measure electrochemical impedance was conducted with an electrochemical system (mod 650C CH-Instrument Inc., TX, USA,). A standard three-electrode system, which employed a platinum wire as counter electrode, Silver/Silver chloride electrode as reference electrode, and a modified Glassy carbon electrode (GCE) as working electrode, respectively. A 200 W Tungsten lamp was utilized as the light source. A 0.1 M Na_2SO_4 aqueous solution was used as the electrolyte. The ZnS QDs modified electrodes were prepared by a simple casting method as follows: 5 µL

ZnS QDs suspension was dropped onto the pretreated GCE and dried in air at room temperature. Nyquist plots were recorded the 1 MHz to 1 kHz frequency range.

2.4. Photocatalytic procedure for the removal of Malachite green

Photocatalytic activity of the samples was evaluated by the photo-degradation of MG under 200 W Tungsten lamp. 0.04 g photocatalysts were added in 100 mL MG (10 mg L^{-1}) in a 500 ml glass beaker. Afterward, the suspensions were magnetically stirred for 30 min in the dark to ensure that the MG could reach the absorption–desorption equilibrium, The irradiation was carried out with a 200 W Tungsten lamp, which was put above beaker. The distance between the solution and lamp was constant, 15 cm, in all experiments with maximum illumination time up to 120 min. At regular time intervals, 2 mL of the samples was taken and analyzed by using UV-Visible spectrophotometer (Agilent 8453 UV-Vis spectrophotometer, USA) at the wavelength of MG at 620 nm). The decrease in the absorbance value of the MG dye after irradiation in a certain time interval is a measure of the dye degradation during the photocatalytic reaction. Furthermore, all experiments were performed at room temperature. In order to evaluate the photocatalytic performance, the degradation rate (D) is calculated from the following equation [26]

$$D = \frac{C_o - C_t}{C_o} X\ 100 = \frac{A_o - A_t}{A_t} X\ 100 \quad \text{---------- (1)}$$

Where

C_o is the initial concentration of MG dye. C_t is the concentration of MG dye after t min.

A_o is the initial absorbance of MG dye. A_t is the absorbance of MG dye after t min.

3 Results and discussion

3.1. Structural Studies

Fig. 1 shows the XRD pattern of all the ZnS QDs samples. The XRD patterns of the prepared samples observed the three characteristic peaks corresponding to (1 1 1), (2 2 0) and (311) planes. The corresponding 2θ peaks were found at 28°, 48° and 56°. The peaks matches well with JCPDS NO 05-566 [27] indicating a cubic crystalline structure of zinc blend. The slight variation in XRD peak position and intensity among the prepared samples were noticed. It indicates that the Ni^{2+} ion dopant and different capping agent have made noticeable effect on the ZnS QDs. By using Debye-Scherrer relation (1) [28], the crystallite size of the ZnS QDs was obtained about 1.2-1.8 nm and shown in Table 1.

$$D = 0.94\lambda / \beta \cos\theta \quad \text{---------- (2)}$$

The capping agent would have restricted the growth of the particle size. The broadening of XRD peaks would illustrated nano size formation of the as prepared samples [28]. The XRD broadening could be also due to contributions of strain (ε). Hence an attempt has been made to estimate the strain of the ZnS QDs samples using Stokes-Wilson equation (2) [29].

$$\text{Strain} = \beta/4\text{Tan}\theta \quad \text{---------- (3)}$$

The values are given in Table.1. The dopant and capping agent had also made distortion in the host which can be seen in the increasing order of strain as the particle size decreases [29].

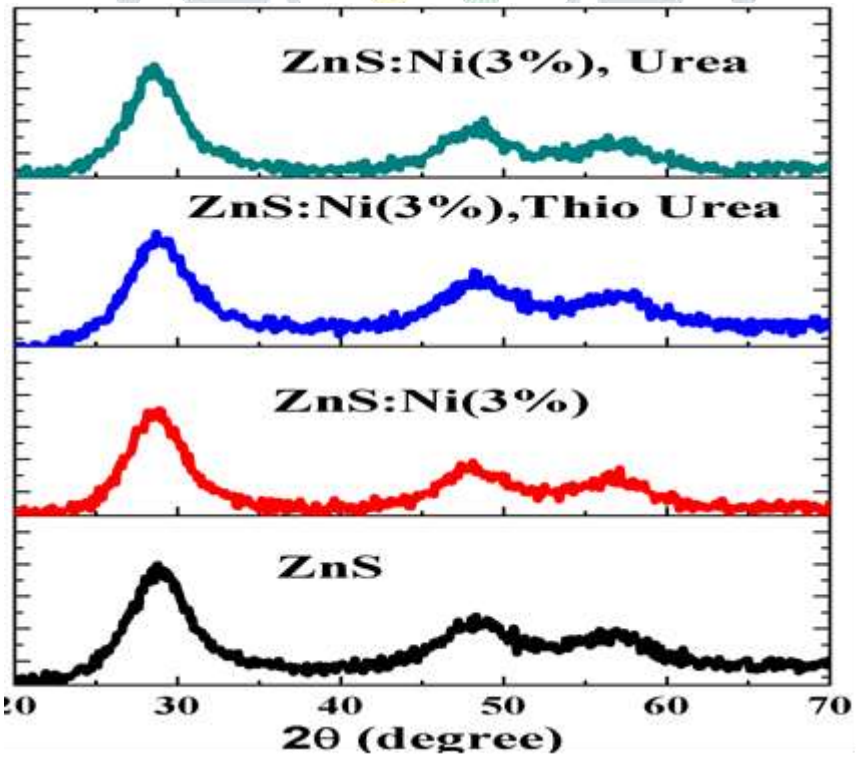

Fig. 1 XRD Pattern for ZnS QDs, ZnS: Ni (3%) QDs, ZnS: Ni(3%): Thiourea QDs, ZnS: Ni(3%): urea QDs

Table 1. Structural parameters of ZnS QDs ZnS: Ni (3%) QDs, ZnS: Ni(3%): Thiourea QDs, ZnS: Ni(3%): urea QDs

S.No	Sample	Particle Size(nm)	Strain
1	ZnS QDs	1.8	0.05425
2	ZnS:Ni (3%) QDs	1.6	0.0577
3	ZnS:Ni (3%) : Thiourea QDs	1.3	0.0725
4	ZnS: Ni (3%): Urea QDs	1.2	0.0733

3.2 Morphological and compositional analysis

Surface morphology of the prepared samples was investigated by using SEM technique. Fig. (2a-5a) shows that the particles of different samples are different shape and nano size. The samples show some distinct modification of surface morphology due the incorporation of different concentration of dopant and different capping agent. The EDAX analysis Fig. 2b-5b confirms that Zn, Ni, S and O elements are present in the respective samples. Hence, it confirms the successful doping of Ni^{2+} ion on the ZnS crystal lattice under different capping agent of thiourea and urea.

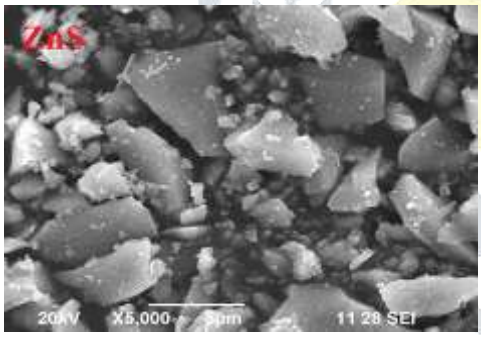

Fig. 2a SEM image of ZnS QDs

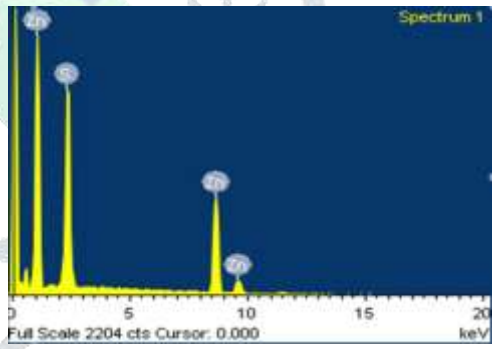

Fig. 2b EDAX image of ZnS QDs

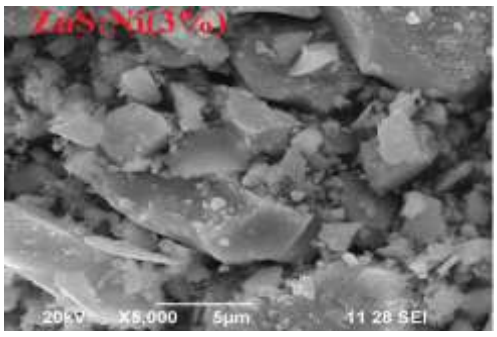

Fig.3a SEM image of Ni(3%): ZnS QDs

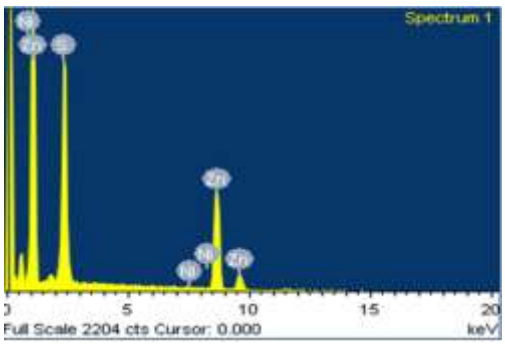

Fig. 3b EDAX image of Ni(3%): ZnS QDs

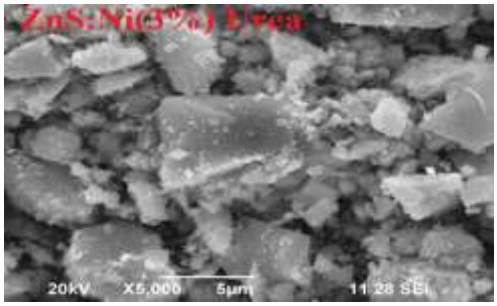

Fig. 4a. SEM image of Urea capped Ni (3%), ZnS QDs

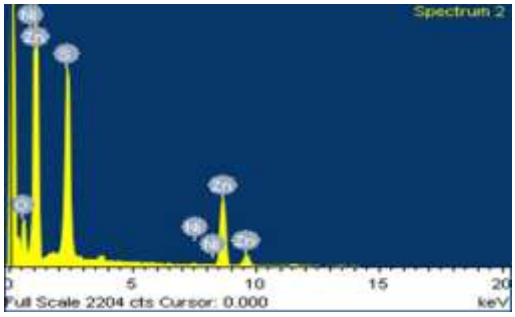

Fig. 4b EDAX image of Urea capped Ni (3%), ZnS QDs

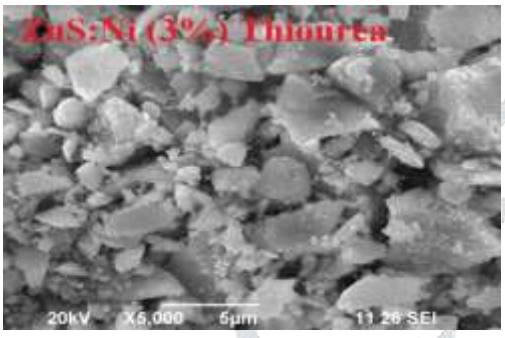

Fig. 5a. SEM image of Thiourea capped Ni (3%): ZnS QDs

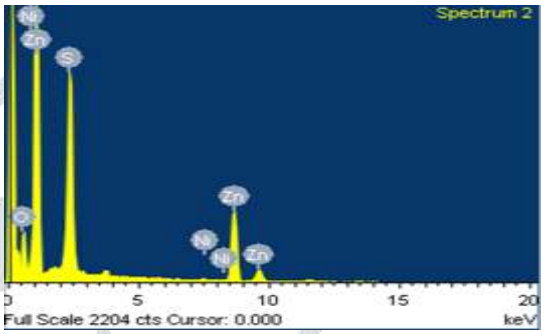

Fig. 5b. EDAX image of of Thiourea capped Ni (3%): ZnS QDs

3.3. FTIR Studies:

FTIR spectra shown in Fig. 6 for samples ZnS QDs, ZnS: Ni (3%) QDs, ZnS: Ni(3%): Thiourea QDs, ZnS: Ni(3%): urea QDs in the range 400–4000 cm^{-1} using JASCO FTIR-410 spectrophotometer. The peaks at 470 cm^{-1}, 617 cm^{-1} and 671 cm^{-1} are assigned to the Zn–S stretching vibration [30]. Shift in the peak position and variation in their intensity were observed in all the doped ZnS QDs samples compared to undoped ZnS QDs with different capping agent. The band at 1010 cm^{-1} is strongly present with broadness due to Zn–S vibration [31]. The broad absorption peaks in the range of 3410–3465 cm^{-1} corresponds to –OH group indicates the existence of water absorbed in the surface of all the ZnS QDs.

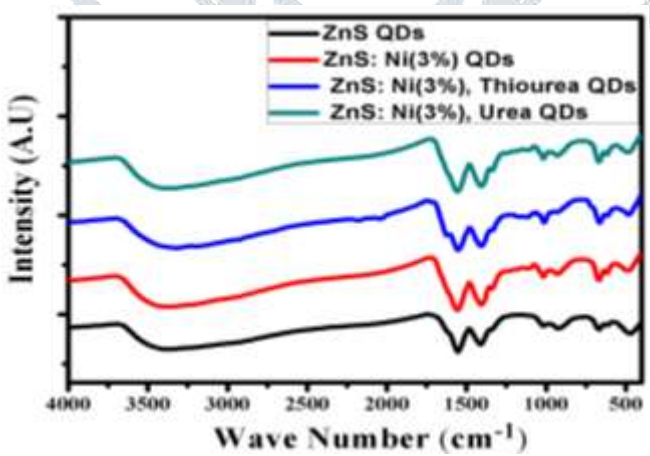

Fig. 6 FTIR spectra of ZnS, ZnS: Ni (3%) QDs, ZnS: Ni(3%): Thiourea QDs, ZnS: Ni(3%):urea QDs

3.4. Optical study

3.4.1. Uv-Visible studies

It is well known that UV–Visible absorption spectra provide good information related to the optical properties, size, and band gap of semiconductor QDs. UV–Vis absorption spectra of all the prepared samples have been observed by using UV-Visible spectrophotometer shown in Fig. 7. From the absorption spectra of ZnS QDs prepared samples, it is clear that strongest absorption edge of the prepared samples is in the range of 293-305nm. The absorption values are found to be blue-shifted from that of the bulk ZnS (345 nm) [32]. A weak absorption peaks were also found around the visible region at 400nm and 750 nm in all the ZnS QDs samples except undoped ZnS QDs. These peaks substantiates that the prepared samples can be used for visible light photocatalytic

reaction. Intensity of Urea capped Ni^{2+} ion doped ZnS QDs samples peaks at 400 nm and 750 nm has found at maximum. This indicates urea capped sample exhibit better performance than other ZnS QDs samples.

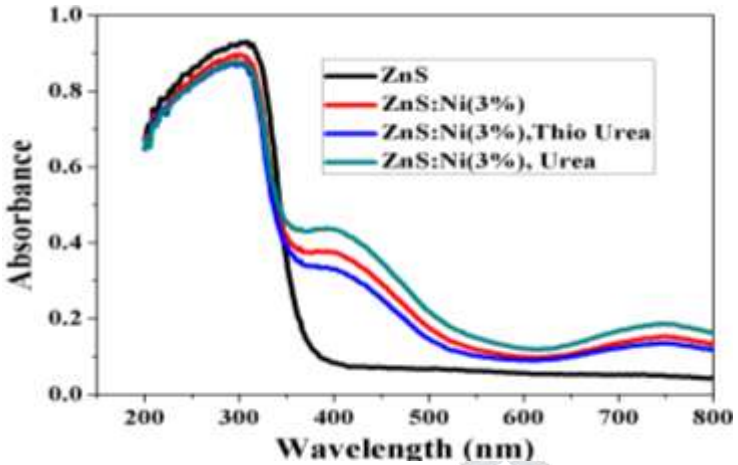

Fig. 7 Optical absorbance spectra for ZnS QDs, ZnS:Ni(3%) QDs , Thiourea capped ZnS:Ni(3%) QDs, urea capped ZnS:Ni(3%)QDs

The band gap for all the samples are calculated using the following equation (3) [33]

$$(\alpha h\nu)^{1/n} = C\,(h\nu - E_g) \quad \text{---------- (4)}$$

where h is the Plank's constant, ν is the photo-frequency, C is a constant, Eg is the band-gap and n depends on the type of transition. The n value for a direct band-gap semiconductor is 1/2, and for an indirect band-gap semiconductor is 2. ZnS is a direct band-gap semiconductor, therefore n=1/2. Thus, the band-gap obtained from the plot of $(\alpha h\nu)^2$ vs hν as shown in the Fig. (8a-8d). The band gap and absorbance values are given in Table 2.The band gap of the undoped ZnS is 3.6 eV and for Ni^{2+} ion doped ZnS QDs is 3.63 eV. The band gap for thiourea and urea capped sample are 3.65 eV and 3.76 eV respectively. Since, the band gap energy of macrocrystalline ZnS is 3.54 eV [32]. The capped samples are exhibiting a red shift; therefore, the enhanced band gap energy can also be related to a decrease in the particle size, which is a result of the quantum size confinement effect [34].

Table 2. Absorbance & Band gap of ZnS QDs, ZnS: Ni (3%) QDs, ZnS: Ni(3%): Thiourea QDs, ZnS: Ni(3%): urea QDs

S.No	Sample	Absorbance (nm)	Band gap (eV)
1	ZnS QDs	293	3.6
2	ZnS:Ni (3%) QDs	294	3.63
3	ZnS: Ni (3%) , Thiourea QDs	299	3.65
4	ZnS: Ni (3%) Urea QDs	305	3.76

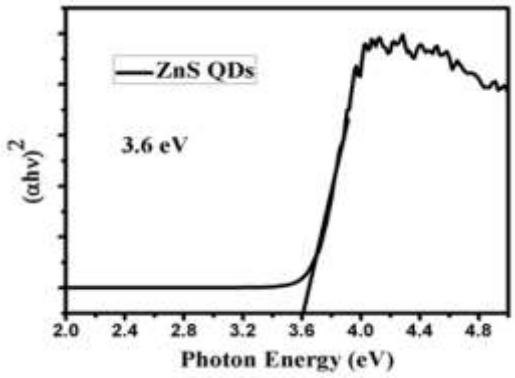

Fig. 8a Plot of $(\alpha h\nu)^2$ versus photon energy of ZnS QDs

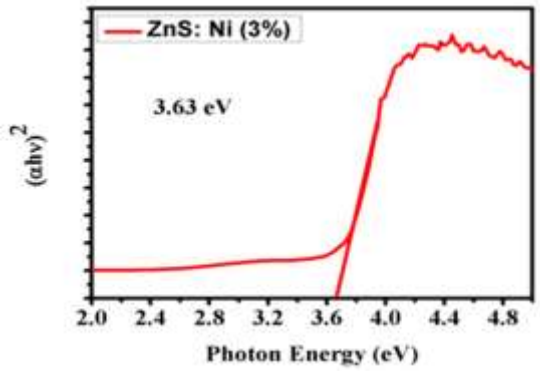

Fig. 8b Plot of $(\alpha h\nu)^2$ versus photon energy of ZnS: Ni (3%) QDs

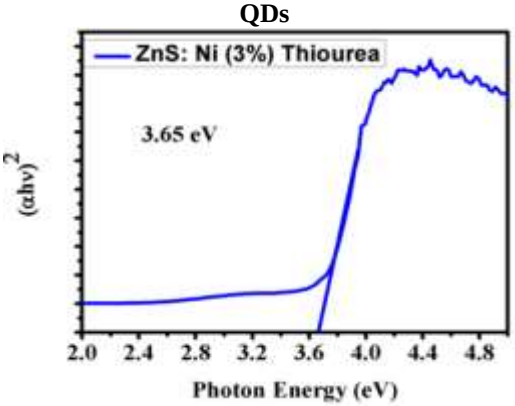

Fig. 8c Plot of $(\alpha h\nu)^2$ versus photon energy of ZnS: Ni(3%): Thiourea QDs

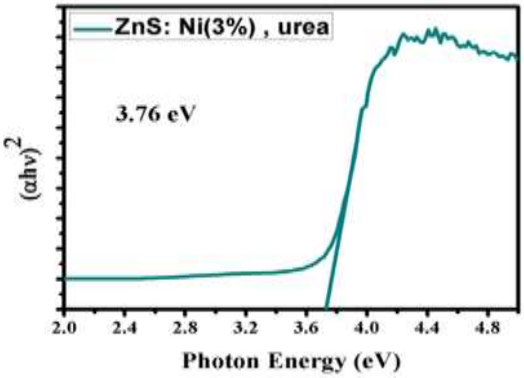

Fig. 8d Plot of $(\alpha h\nu)^2$ versus photon energy of ZnS: Ni(3%): urea QDs

The photocatalytic activity of photocatalysts is affected by their band gap energy. Larger band gap energy leads to higher redox potential of electron-hole pairs and consequently the higher photocatalytic activity [35].

3.4.2 PL Study

PL spectrum of prepared ZnS QDs samples show a narrow maximum emission peaks at 387 nm, 521 nm and 789 nm when excited at 330 nm. The appearance of a narrow emission spectrum of the Photo-luminescent materials is a sign of the presence of high degree of monodispersity. Furthermore, the emission band in the PL spectrum of ZnS QDs at about 387 nm could be assigned to the deep level states such as dislocations, interstitials and Zn^{2+} vacancies [36].

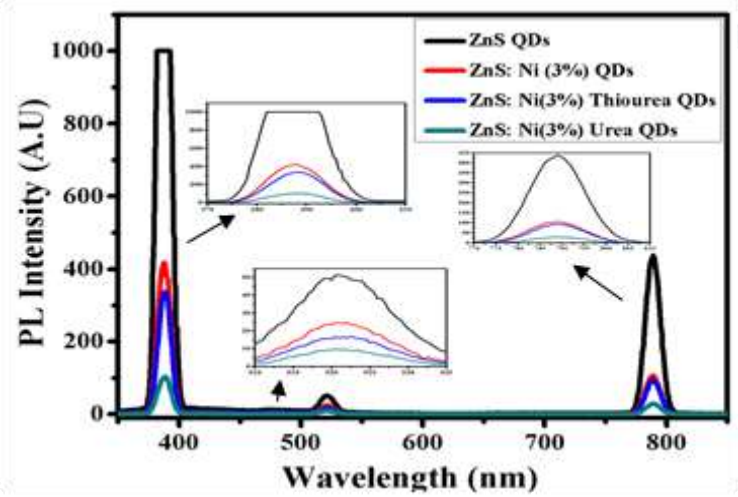

Fig. 9 Photoluminescence spectra of ZnS QDs, ZnS: Ni (3%) QDs, ZnS: Ni(3%): Thiourea QDs, ZnS: Ni(3%): urea QDs

Emission band in the PL spectrum of ZnS QDs at about 520 nm is assigned due to dopants and impurity atoms where transitions occur from the conduction band of ZnS QDs to the different excited levels of the impurity atoms and dopants in the ZnS band gap. The emission band in the PL spectrum of ZnS QDs at about 789 nm which falls on the red region produced by ZnS QDs

has suitable for fabricating near-infrared light-emitting Devices. Fig. 9 shows the PL spectra of different ZnS QDs samples. The PL values are given Table 3. The intensity of the emission band decreases significantly when the ZnS QDs is doped with Ni and further the PL intensity decreases when the Ni doped ZnS QDs is capped with thiourea and urea. Among the two capping agent, urea capped Ni (3%):ZnS QDs has lowest intensity, which is due to the lowering of the recombination probability of photo excited charge carriers followed by efficient transfer of photo excited electrons for decomposition of MG dye and enhanced the photocatalytic activities.

Table 3. PL Peak wavelength and Intensity

S.No	Sample	Peak Wavelength (nm)	Peak Intensity	Peak Wavelength (nm)	Peak Intensity	Peak Wavelength (nm)	Peak Intensity
1	ZnS QDs	387.5	999.99	521	51.26	789	437.18
2	ZnS:Ni (3%) QDs	388	417.86	522	24.747	789.5	106.25
3	ZnS:Ni(3%): Thiourea QDs	388.5	337.56	522.5	16.854	789.5	92.676
4	ZnS: Ni(3%):Urea QDs	388.5	104.21	520.5	9.85	788.5	29.24

3.5 Electrochemical Study

To understand the role different prepared ZnS QDs samples towards photocatalytic degradation in a better way, Nyquist plots obtained through electrochemical impedance spectroscopy (EIS) were plotted. As shown in Fig. 10, the Nyquist impedance plots for undoped ZnS QDs, Ni doped ZnS QDs , Thiourea & urea capped Ni doped ZnS QDs modified GCE electrode materials cycled in 0.1 M Na_2SO_4 electrolyte solution exhibit semicircles at high frequencies in presence of visible irradiation.

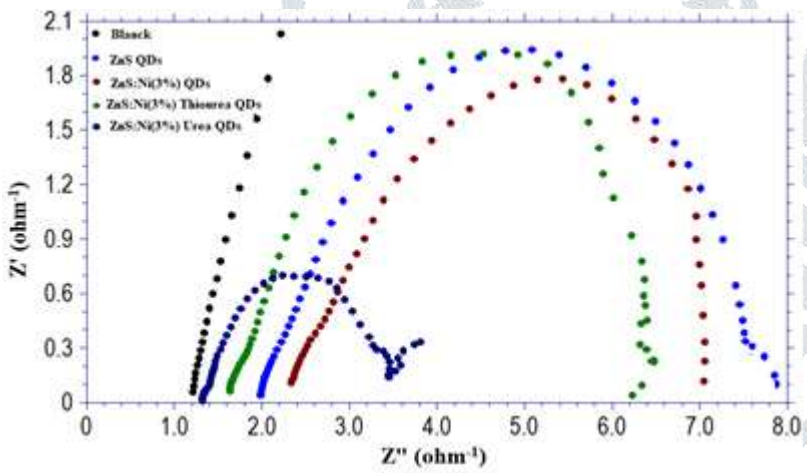

Fig. 10 Nyquist (impedance) plots of Blank GCE, ZnS QDs, ZnS : Ni(3%) QDs, ZnS:Ni(3%): Thiourea QDs, ZnS:Ni(3%): urea QDs modified GCE electrodes.

The arc radius of the EIS Nyquist plot of Urea capped sample are found to be smaller than that of rest of the samples, suggesting that charge transfer is more in urea capped sample [37]. A smaller arc radius of the EIS Nyquist plot was observed under visible-light irradiation for urea capped ZnS: Ni(3%) sample which indicates a more effective separation efficiency of photogenerated electron–hole pairs and a faster interfacial charge transfer [38]. This result implies that the urea capped sample has brought an appreciable change in the electrochemical behaviour of ZnS QDs. Thus inclusion of Ni^{2+} dopant and Urea capping agent into the ZnS lattice substantially improve the photocatalytic activity.

3.6 Photocatalytic studies

Photocatalytic degradation of MG dye was conducted to investigate the combined effect of doping and capping agent on photocatalytic activity of ZnS QDs. Spectral changes indicates the absorbance of dye during photochemical reaction catalysed by ZnS QDs, ZnS: Ni (3%) QDs, ZnS: Ni(3%): Thiourea QDs, ZnS: Ni(3%): urea QDs. The characteristic absorption peak of this dye at 620 nm was selected to monitor the photocatalytic degradation of the dye. By Beer Lambert law, the decrease in concentration of dye was recorded at different intervals of time to measure degradation rate. Fig. 11(a-d) shows the change in absorbance of MG dye exposed to visible light for various irradiation times (0 min, 30 min, 60 min, 90 min and 120 min) in the presence of different prepared ZnS QDs samples at 620 nm was found and it decreased gradually with time.

The result reveals that the Urea and Thiourea capped ZnS QDs samples showed higher photocatalytic activity than that of Ni doped ZnS and undoped ZnS QDs. They showed photo-catalytic activity with a degradation efficiency of 81% and 79% for MG respectively. The increased percentage of dye degradation confirms the efficient degradation of MG during photocatalytic reaction. Therefore, combined effect of capping agent and dopant has a significant effect on ZnS QDs leading improved photocatalytic activity by enhancing the electron–hole separation in the photocatalyst surface. Photo-catalytic activity degradation of ZnS QDs and Ni doped ZnS QDs was found to be 68% and 75% respectively. The plot of the percentage of photodegradation against time is shown in Fig. 12 for undoped, Ni doped and capping agent (Thiourea & urea) coated on Ni doped photocatalyst under visible light illuminations. The photodegradation efficiency of the catalyst increases when Ni^{2+} dopant and urea capping agent were incorporated in to the ZnS QDs. This is due to formation of defects states due to combined effect of dopant and capping agent [39]. In the present study Urea capped Ni doped ZnS QDs was found comparatively higher degradation efficiency than the other prepared ZnS QDs samples.

Table 4. Percentage Dye degradation of ZnS QDs, ZnS : Ni(3%) QDs, ZnS:Ni(3%): Thiourea QDs, ZnS:Ni(3%): urea QDs

S.No	Name of the sample	% Dye Degration
1	ZnS QDs	68
2	ZnS:Ni (3%) QDs	75
3	ZnS:Ni (3%) :Thio urea QDs	79
4	ZnS:Ni (3%) :urea QDs	81

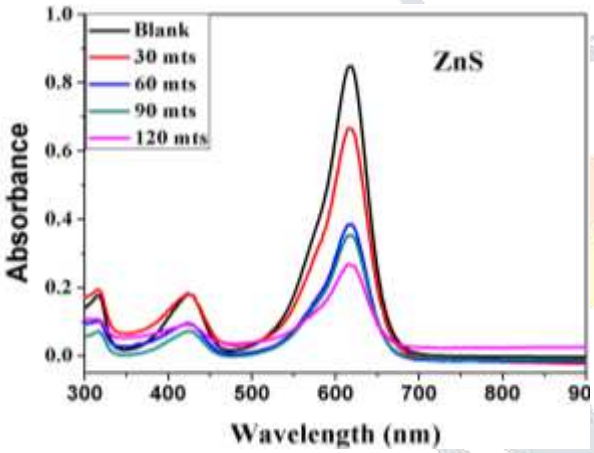

Fig 11a. UV–visible spectral changes of MG with reaction time in the presence of ZnS QDs under visible light.

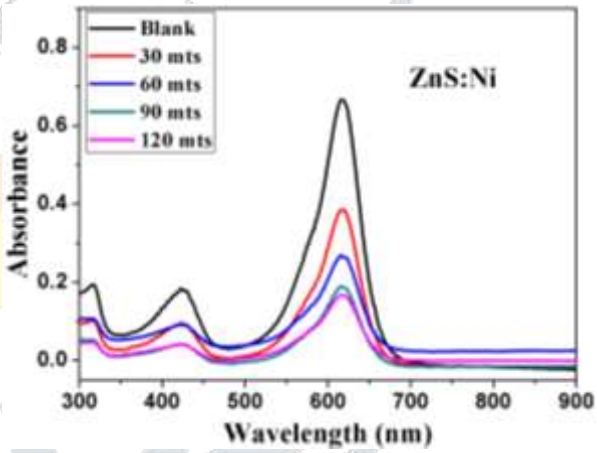

Fig 11b. UV–visible spectral changes of MG with reaction time in the presence of ZnS:Ni(3%) QDs under visible light.

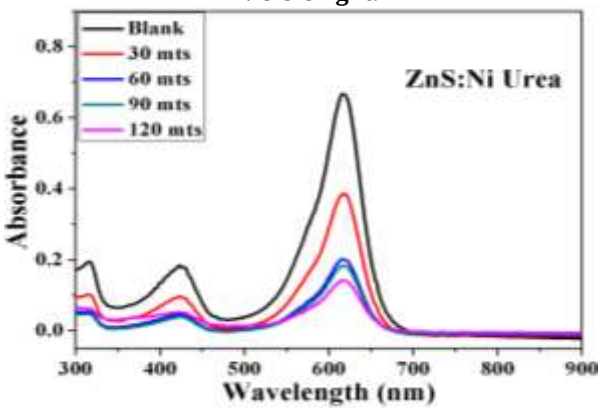

Fig 11c. UV–visible spectral changes of MG with reaction time in the presence of urea capped ZnS: Ni(3%) QDs under visible light

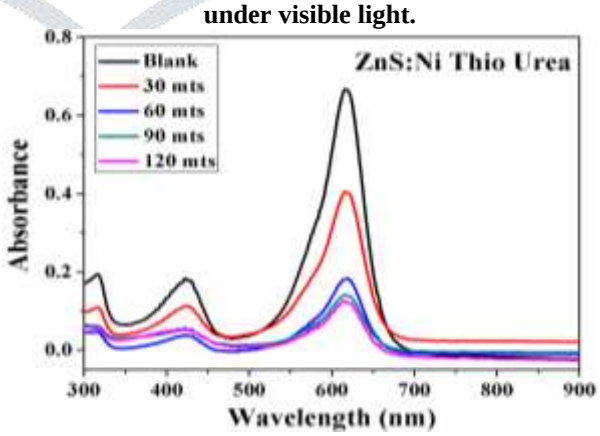

Fig 11d. UV–visible spectral changes of MG with reaction time in the presence of Thio urea capped ZnS: Ni(3%) QDs under visible light.

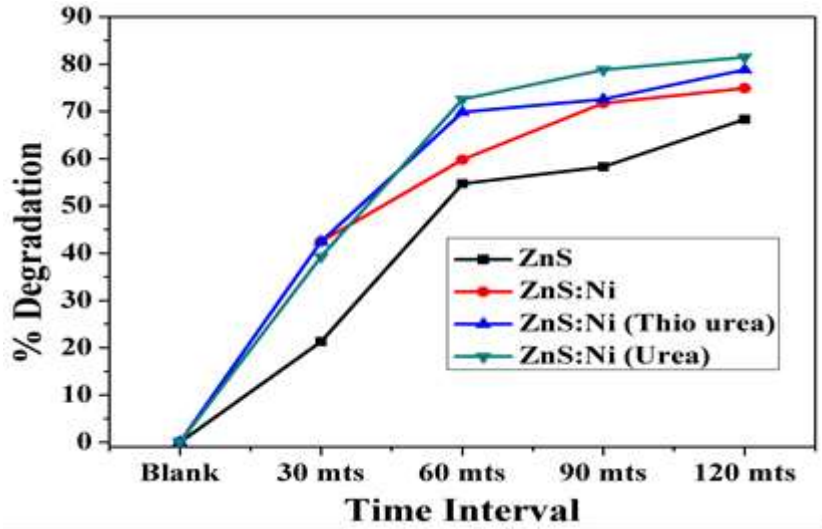

Fig 12. Linear plots for the photodegradation of MG under visible light in the presence of ZnS QDs, ZnS:Ni(3%) , Thiourea capped ZnS:Ni(3%) , urea capped ZnS:Ni(3%)QDs

4. Conclusion

In recent years, QDs based photocatalytic methods are more useful for the removal of organic pollutants due to some advantages such as: long-term stability, large retention capability and more efficiency for the pollutant remediation using only a small amount of QDs nanophotocatalysts. In this work, a QDs based photocatalytic degradation process has been presented as an efficient, simple and green strategy for the removal of dye pollutant. The structural and optical properties of pure ZnS QDs, Ni doped QDs , Thiourea and urea capped Ni doped ZnS QDs have also been characterized by XRD, SEM, UV–Vis absorption and Photoluminescence techniques. According to the results, urea acted as an effective capping agent along with Ni^{2+} dopant for the preparation of ZnS QDs. EIS studies indicates that respective QDs sample exhibited as a superior electrochemical catalyst which acts as supporting evidence to the positive impact of the increase in photo catalytic activity due to the combined effect of Ni dopant and urea capping agent on ZnS QDs.

Reference:

1. A. M. Smith, S. Nie, Semiconductor NCs: structure, properties, and band gap engineering, Acc. Chem. Res. 43 (2009) 190-200.
2. P. Kambhampati, Hot exciton relaxation dynamics in semiconductor quantum dots: radiationless transitions on the nanoscale, J. Phys. Chem. C, 115 (2011) 22089-22109.
3. J. Biener, A. Wittstock, T. F. Baumann, J. Weissmüller, M. Bäumer & A. V. Hamza, Surface chemistry in nanoscale materials, Materials, 2 (2009) 2404-2428
4. Y. Shu, B. Fales, W. T. Peng, & B. G. Levine, Understanding Nonradiative Recombination through Defect-Induced Conical Intersections, J. Phys. Chem. Lett., 8 (2017) 4091-4099.
5. J. Schneider, M. Matsuoka, M. Takeuchi, J.Zhang, Y. Horiuchi, M. Anpo & D. W. Bahnemann, Understanding TiO_2 photocatalysis: mechanisms and materials. Chemical reviews, 114 (2014) 9919-9986.
6. K. Rajeshwar, N.R. de Tacconi, C. R. Chenthamarakshan, Semiconductor-based composite materials: preparation, properties, and performance, Chem. Mater. 13 (2001) 2765-2782.
7. F.J. Heiligtag, M. Niederberger, The fascinating world of nanoparticle research, Mater. Today, 16 (2013) 262-271.
8. M. Z. Hu, & T. Zhu, Semiconductor nanocrystal quantum dot synthesis approaches towards large-scale industrial production for energy applications, Nanoscale Res. Lett., 10 (2015) 469-474.
9. R. Sharma, Structural and optical characterization of ZnS NPs, Int. J. Multidiscip. Res., 1 (2011) 8-11.
10. Q. Zhou, J. Z. Wen, P. Zhao, W. A. Anderson, Synthesis of vertically-,aligned Zinc oxide nanowires and their application as a photocatalyst, Nanomaterials, 7 (2017) 1-13.
11. A. Termeh Yousefi, N. A. Kadri, Morphology optimization of highly oriented carbon nanotubes for bioengineering applications, Mater Res Innov. 20 (2016) 268-271.
12. N. Shanmugam, B. Saravanan, R. Reagan, N. Kannadasan, K. Sathishkumar, S. Cholan, Effect of Thermal Annealing on the Cd(OH)2 and Preparation of CdO NCs, Mod. Chem. Appl, 2 (2014) 1-5.
13. A. M. Mostafa, S. A. Yousef, W. H. Eisa, M.A Ewaida, E. A. Al-Ashkar, Synthesis of cadmium oxide NPs by pulsed laser ablation in liquid Environment, Optik, 144 (2017) 679-684.
14. L. Qi, H. Cölfen, M. Antonietti, Synthesis and characterization of CdS NPs stabilized by double-hydrophilic block copolymers, Nano Lett. 1 (2001) 61-65.
15. B. Kaur, K. Singh, A.K Malik, Effect of ligands on crystallography, morphology and photo-catalytic ability of ZnS nanostructures. Dyes and Pigments, 142, (2017) 153-160.
16. Lokteva, N. Radychev, F. Witt, H. Borchert, J. Parisi, J. Kolny-Olesiak, Surface treatment of CdSe NPs for application in hybrid solar cells: the effect of multiple ligand exchange with pyridine, J Phys Chem Lett. 114 (2010) 12784-12791.
17. C. Y. Chen, G. Zhu, Y. Hu, J. W. Yu, J. Song, K. Y. Cheng, Z. L. Wang, Gallium nitride nanowire based

nanogenerators and light-emitting diodes, ACS nano, 6 (2012) 5687-5692.
18. N. Kaur, S. Kaur, J. Singh, M. Rawat, A Review on Zinc Sulphide NPs: From Synthesis, Properties to Applications, J. Bioelectron Nanotechnol. 1 (2016) 1-5.
19. D. Bera, L. Qian, T. K. Tseng, P. H. Holloway, Quantum dots and their multimodal applications: a review, Materials, 3 (2010) 2260-2345.
20. A. M. Sajimol, A. Roselin, V. G. Sreevalsa, G. D. Deepa, G. Bhat Sarita, S. Jayalekshmi, Highly luminescent and biocompatible, l-citrulline-capped ZnS: Mn NCs for rapid screening of metal accumulating Lysinibacillus fusiformis bacteria, Luminescence, 28 (2013) 461-467.
21. P. Yang, M. Lü, D. Xü, D. Yuan, C. Song, G. Zhou, The effect of Co^{2+} and Co^{3+} on photoluminescence characteristics of ZnS nanocrystallines',J. Phys. Chem. Solids, 62 (2001) 1181-1184.
22. T. M. Thi, L. Van Tinh, B. H. Van, P. Van Ben, V. Q. Trung, The effect of polyvinylpyrrolidone on the optical properties of the Ni-doped ZnS nanocrystalline thin films synthesized by chemical method, J. Nanomater. 528047 (2012) 1-8.
23. G. Murugadoss & V. Ramasamy, Luminescence study of monodispersed ZnS NPs. Luminescence, 28 (2013) 195-201.
24. J. S. Hu, L. L. Ren, Y. G. Guo, H. P. Liang, A. M. Cao, L. J. Wan, C. L. Bai, Mass production and high photocatalytic activity of ZnS nanoporous NPs, Angew. Chem.117 (2005) 1295-1299.
25. F. Yu, Y. Chen, X. Liang, J. Xu, C. Lee, Q. Liang, T. Deng, Dispersion stability of thermal nanofluids, Pro Nat S Mater, 27 (2017) 531-542.
26. J. H. Xiao, W.Q. Huang, Y. S. Hu, F. Zeng, Q. Y. Huang, B. X. Zhou, G. F. Huang, Facile in situ synthesis of wurtzite ZnS/ZnO core/shell heterostructure with highly efficient visible-light photocatalytic activity and photostability, J. Phys. D: Appl. Phys. 51 (2018) 1-26.
27. G. Murugadoss & V. Ramasamy, Luminescence study of monodispersed ZnS NPs. Luminescence, 28 (2013) 195-201.
28. R. K. Srivastava, N. Pandey, S. K. Mishra, Effect of Cu concentration on the photoconductivity properties of ZnS NPs synthesized by co- precipitation method'. Mater. Sci. Semicond. Process, 16 (2013) 1659-1664.
29. M. S. Al-Kotb, J. Z. Al-Waheidi, M. Kotkata, Investigation on microstructural and optical properties of nano-crystalline CdSe thin films, Thin Solid Films, 631 (2017) 219-226.
30. M. M. Farooqi, R. K. Srivastava, Structural, optical and photoconductivity study of ZnS NPs synthesized by a low temperature solid state reaction method, Mater. Sci. Semicond. Process, 20 (2014) 61-67.
31. V. Ramasamy, K. Praba, G. Murugadoss, Study of optical and Thermal properties in nickel doped ZnS NPs using surfactants, Superlattices Microstruct. 51 (2012) 699-714.
32. E. K. Goharshadi, R. Mehrkhah, P. Nancarrow, Synthesis, characterization, and measurement of structural, optical, and phtotoluminescent properties of zinc sulfide quantum dots, Mater. Sci. Semicond. Process, 16 (2013) 356-362.
33. P. Sakthivel, S. Muthukumaran, & M. Ashokkumar, Structural, band gap and photoluminescence behaviour of Mn-doped ZnS quantum dots annealed under Ar atmosphere. Journal of Materials Science: Materials in Electronics, 26 (2015) 1533-1542.
34. M. Roushani, M. Shamsipur & H. R. Rajabi, Highly selective detection of dopamine in the presence of ascorbic acid and uric acid using thioglycolic acid capped CdTe quantum dots modified electrode, J. Electroanal. Chem., 712 (2014) 19-24.
35. M. A. Behnajady , Y. Tohidi, Synthesis, Characterization and Photocatalytic Activity of Mg Impregnated ZnO-SnO_2 Coupled NPs, Photochem. photobiol. 90 (2014) 51-56.
36. M. Sookhakian, Y.M. Amin, W. J. Basirun, M. T. Tajabadi, N. Kamarulzaman, Synthesis, structural, and optical properties of type-II ZnO–ZnS core-shell nanostructure, J. Lumin, 145 (2014) 244-252.
37. Y. Zhang, R. Wen, D. Guo, H. Guo, J. Chen, Z. Zheng, One-step facile fabrication and photocatalytic activities of ZnS@ g-C_3N_4 nanocomposites from sulfatotris (thiourea) zinc (II) complex, Appl. Organomet. Chem. 30 (2016) 160-166.
38. Y. Li, X. He, M. Cao, Micro-emulsion-assisted synthesis of ZnS nanospheres and their photocatalytic activity. Mater. Res. Bull. 43 (2008) 3100-3110.
39. S. Anandan, Y. Ikuma, K. Niwa, An overview of semi-conductor photocatalysis: modification of TiO_2 nanomaterials, Solid State Phenom. 162 (2010) 239-260.